

The calculation of the muon transfer rate from protium to neon on the ground of a two-centre Coulomb basis

S. V. Romanov^{1, 2, *}

¹*National Research Centre "Kurchatov Institute", Moscow, 123182, Russia.*

²*Moscow Institute of Physics and Technology, Moscow, 123098, Russia.*

The results of improved calculations of the muon transfer rate from the $1S$ -state of muonic protium to neon are presented in the interval of collision energies from 10^{-4} eV to 15 eV. The calculations have been made within the perturbed stationary states method in which the wavefunction of the three-body system (muon, proton and neon nucleus) is expanded in eigenfunctions of a two-centre Coulomb problem formulated in the Jacobi coordinates of the entrance channel. This approach provides the asymptotically correct description of the entrance channel. Namely, the correct dissociation limit is obtained, there are no spurious long-range interactions, the polarization attraction between muonic protium and neon appears naturally. Moreover, the electron screening, which is important at low collision energies, can be easily taken into account. The defects of the description are removed into the muon transfer channel in which their effect is not expected to be too significant because of large energies of the relative motion in this channel. The previous calculations carried out in this way allowed one to explain experimentally observed features of the temperature dependence of the transfer rate in hydrogen-neon mixtures. In the present work, a more perfect algorithm of constructing the basis eigenfunctions of the two-centre Coulomb problem has been realized and a better agreement with experimental data has been obtained.

PACS numbers: 34.70.+e, 36.10.Ee

1. INTRODUCTION

The direct muon transfer from protium to neon is considered in the present paper. It is a particular case of the charge transfer from muonic protium μp ($1S$) in its ground state to a chemical element with the atomic number Z :



Here μZ^* is the muonic atom of the element Z in an excited state. The rate $\lambda(T)$ of the muon transfer from thermalized μp atoms was measured in liquid hydrogen-neon mixtures at the temperature $T = 20$ K [1] and in dense gaseous mixtures at $T = 300$ K [2]. The corresponding results traditionally reduced to the atomic density of liquid hydrogen $N_H = 4.25 \times 10^{22} \text{ cm}^{-3}$ are given in Table 1. The most interesting feature of the reaction considered is its anomalously small rate at room temperature. It is an order of magnitude less than the muon transfer rate to other elements

*Romanov.SVi@nrcki.ru; Serguei.V.Romanov@gmail.com

Table 1: The experimental λ_e and calculated λ_t values of the rate $\lambda(T)$ of the muon transfer from thermalized $\mu p(1S)$ atoms to neon for two values of the temperature T . All the rates are given in units of 10^{10} s^{-1} and reduced to the atomic density of liquid hydrogen. Three values of the transfer rate given in two columns correspond to the cases A, B, and C of taking into account the electron screening.

$T, \text{ K}$	λ_e [1, 2]	λ_t			
		[3]	[5]	[12]	the present work
20	3.00 ± 1.00	–	6.40 (A)	1.2	2.48 (A)
			1.30 (B)		0.81 (B)
			3.56 (C)		2.00 (C)
300	0.849 ± 0.018	0.4	3.31 (A) 1.36 (B) 2.02 (C)	1.02	1.62 (A) 0.87 (B) 1.25 (C)

with $Z \geq 6$ [1]. Moreover, the temperature dependence of the transfer rate is of interest. Indeed, as the temperature is increased from 20 K to 300 K, $\lambda(T)$ falls by a factor of three. This means that the standard v^{-1} dependence of the transfer cross-section on the relative velocity v is incorrect at collision energies corresponding to room temperature.

The first attempt to explain the anomalously small value of the transfer rate at room temperature was made by Sayasov [3]. A traditional way of calculating the rate of the reaction (1) is based on consideration of quasicrossings of adiabatic terms correlated to states of the muonic atoms $\mu p(1S)$ and μZ^* . Then the Landau-Zener formula is used to estimate probabilities of transitions between these terms [4]. Sayasov pointed to the fact that, in the case of the muon transfer to light elements, the WKB approximation is not applicable in quasicrossing regions. Therefore, the standard Landau-Zener formula is also not applicable. Having modified it in a proper way, Sayasov obtained the transfer rate in the form of an oscillating function whose argument depends on Z , the mass of the hydrogen isotope, and the coordinate of the relevant quasicrossing point (the two-state approximation was used and only the S -wave was considered). For the muon transfer from protium to neon, the value of the argument proved to be close to the position of a minimum of the function and the estimated value of the transfer rate was found to be two times less than the experimental value (Table 1). Concerning the decrease of the transfer rate in the temperature interval 20–300 K, it remained unexplained. The standard v^{-1} law was obtained for the transfer cross-section. This means that the transfer rate does not depend on v and, consequently, it is independent of temperature.

The next step was made in the work [5]. It was carried out in connection with the experiment [6] on the laser excitation of the $2S - 2P$ transition in muonic protium with the aim of a precise determination of the mean-square charge radius of the proton. The muon transfer from the metastable $2S$ -state of muonic protium to neon was considered as a way of detecting this state [7, 8]. In this case, the muon transfer from the $1S$ -state is a background and it is desirable to know the energy dependence of its rate. In ref. [5] this rate was calculated in the interval of collision energies from

10^{-4} eV to 15 eV. The lowest value corresponds to the temperature about 1 K, the uppermost one is close to the lowest electron excitation energy of neon (16.6 eV [9]). The method of calculations was based on the substantial difference in energies of the relative motion in reaction channels. In the entrance channel ($\mu p(1S) + \text{Ne}$) the collision energy does not exceed 15 eV, whereas in the transfer channel ($\mu \text{Ne}^* + p$) it is a few keV [2]. It is obvious that an asymptotically correct description of the entrance channel is of primary importance in this case. Accordingly, the wave function of the three-body system was constructed as an expansion in eigenfunctions of a two-centre Coulomb problem formulated in the Jacobi coordinates of the entrance channel. As a result, the correct dissociation limit is obtained in this channel, no spurious long-range interactions arise, and the polarization attraction between muonic protium and neon appears naturally. Moreover, even in the simplest approximation the dipolar polarizability of muonic protium is reproduced with one percent accuracy. It is also significant that the electron screening in the entrance channel can be easily taken into account. It proves to be important at low collision energies.

A disadvantage of this approach is that the transfer channel is described in unnatural coordinates (in the Jacobi coordinates of the entrance channel). The eigenstates of the two-centre problem localized at the neon nucleus in the separated atoms limit are not eigenstates of the Hamiltonian of isolated muonic neon. Nevertheless, the inclusion of a group of such states in calculations allows one to describe the migration of the muon from protium to neon. It is obvious that no partial transfer rates to individual states of the final μNe^* atom can be obtained in this way. However, the total transfer rate can be evaluated. Although the asymptotic description of the transfer channel shows a number of defects (incorrect dissociation limits, spurious long-range interactions), their effect is not expected to be too significant because of large energies of the relative motion in this channel. In truth, the method employed in ref. [5] is a variant of the well-known perturbed stationary states (PSS) method. However, unlike its standard realization [10] in which all the binary channels are described incorrectly in asymptotic domains, the above approach provides the asymptotically correct description of the entrance channel with low collision energies and removes all the difficulties into the muon transfer channel.

The calculation made in ref. [5] with four basis eigenfunctions of the two-centre problem recognized some features of the muon transfer from protium to neon.

1. The transfer rate treated as a function of the collision energy has a well pronounced minimum at thermal energies ($T = 300$ K). This corresponds to the above-mentioned strong suppression of the transfer reaction at room temperature.
2. At the same energies the contribution of the P -wave to the transfer rate becomes significant (20–30 %). At the subsequent energy growth, the contributions of waves with greater angular momenta increase rapidly. This leads to the transfer rate going up at energies greater than 0.1 eV. In particular, a resonance peak appears at collision energies of 0.3–0.5 eV. It is due to the existence of a quasi-steady state in the D -wave. It should be noted that only the S -wave was considered in most of earlier calculations.

3. The electron screening in the entrance channel proves to be important at the collision energies less than 1 eV. In order to clarify its role, the calculations were made for the following three cases.

- A) The electron screening was fully ignored. This corresponds to the muon transfer to a bare neon nucleus. The interaction of muonic protium with neon at large separations was described with the help of the ordinary potential of the polarization attraction.
- B) The screening of the nuclear charge of neon by atomic electrons was taken into account in the polarization potential.
- C) A contact interaction of muonic protium with the electron shell of neon was added to the screened polarization potential. This interaction is due to the finite size of muonic protium, and it is proportional to the product of the mean-square charge radius of $\mu p(1S)$ and the electron density of neon. It leads to an additional attraction. This case is most realistic because the electron screening is taken into account in a maximum degree.

After averaging over the Maxwellian distribution, the rate $\lambda(T)$ of the muon transfer from thermalized μp atoms was obtained. Its values for the temperatures of 20 K and 300 K are given in Table 1. Attention should be paid to the strong dependence of the results on the way of considering the electron screening. In passing from the case A to the case B, the attraction in the entrance channel becomes weaker and the transfer rate decreases. This is most noticeable at low temperatures. The additional attraction in the case C leads to the transfer rate increasing. Concerning the agreement with experimental data, it is good at $T = 20$ K in the most realistic case C. Of course, it is necessary to note that in a liquid hydrogen-neon mixture the electron screening may be more complicated than it was assumed in the calculation. Moreover, the Maxwellian distribution seems to be a too crude model in this case. At $T = 300$ K the agreement is worse: the transfer rate calculated in the case C exceeds the experimental value by a factor of 2.3. Nevertheless, the calculation correctly reproduces the tendency to decreasing the transfer rate with increasing the temperature. It is interesting that the transfer rate calculated in the case B is nearly constant in the interval 20–300 K, although the agreement with the experimental data at room temperature is better.

After the paper [5] had come out, the results of calculations made within a hyperspherical elliptic coordinates method were published [11, 12]. The values of the muon transfer rate from protium to neon obtained in these works are also given in Table 1. Having included more than one hundred basis functions in the calculation, the authors obtained a very good result. Namely, the observed value of the transfer rate at room temperature was reproduced with the accuracy of 15 %. The agreement with the experimental data at $T = 20$ K is worse: the calculated value of the transfer rate is less than a half of the observed value. Moreover, the transfer rate is nearly constant in the temperature interval considered. It is important to note that the electron screening was fully ignored in this calculation, i.e. the muon transfer to the bare neon nucleus was considered.

Introducing the screening may noticeably reduce calculated values of the transfer rate. For example, according to ref. [13], at room temperature the electron screening reduces the transfer rate by a factor of $Z^{1/3}$, i.e. nearly in half for neon. Such a reduction has been demonstrated in ref. [5] in passing from the case A to the case B.

This paper is a sequel to the work [5]. It presents the results of calculations made within the same approximations but improved in one point. Namely, a more perfect algorithm of constructing the basis eigenfunctions of the two-centre Coulomb problem has been realized.

2. DESCRIPTION OF THE METHOD

As the calculation method has been detailed in ref. [5], only its main points will be briefly considered here. Unless otherwise specified, muon-atom units (m.a.u. for short) are used below:

$$\hbar = e = m_\mu = 1, \quad (2)$$

e is the proton charge, m_μ is the muon mass; the length and energy units are respectively equal to 2.56×10^{-11} cm and 5.63 keV.

Let us consider the system consisting of a negative muon μ , a nucleus H of a hydrogen isotope, and a nucleus with the atomic number Z . Let us introduce the Jacobi coordinates of the entrance channel of the reaction (1): the vector \mathbf{r} connecting the nucleus H with the muon and the vector \mathbf{R} joining the centre of mass C_2 of muonic hydrogen μH and the nucleus Z (Fig. 1). The centre of mass C_3 of the three-body system lies on the vector \mathbf{R} . In the centre-of-mass frame the Hamiltonian of this system is:

$$\hat{H} = -\frac{1}{2M_r} \Delta_{\mathbf{R}} + \hat{H}_\mu + \frac{Z}{R_{\text{HZ}}}. \quad (3)$$

The first term is the operator of the kinetic energy of the relative motion of muonic hydrogen and the nucleus Z . M_r is the reduced mass of the nucleus Z with respect to muonic hydrogen:

$$M_r^{-1} = (M_{\text{H}} + 1)^{-1} + M_Z^{-1}, \quad (4)$$

M_{H} and M_Z are the nuclear masses. \hat{H}_μ is the Hamiltonian of muonic hydrogen with the addition of the Coulomb attraction of the muon and the nucleus Z :

$$\hat{H}_\mu = -\frac{1}{2m_{\mu\text{H}}} \Delta_{\mathbf{r}} - \frac{1}{r} - \frac{Z}{r_{\mu Z}}, \quad (5)$$

$m_{\mu\text{H}}$ is the reduced mass of muonic hydrogen:

$$m_{\mu\text{H}}^{-1} = M_{\text{H}}^{-1} + 1, \quad (6)$$

$r_{\mu Z}$ is the distance between the muon and the nucleus Z . The last term in the formula (3) is the Coulomb repulsion of the nuclei H and Z , R_{HZ} is the internuclear distance.

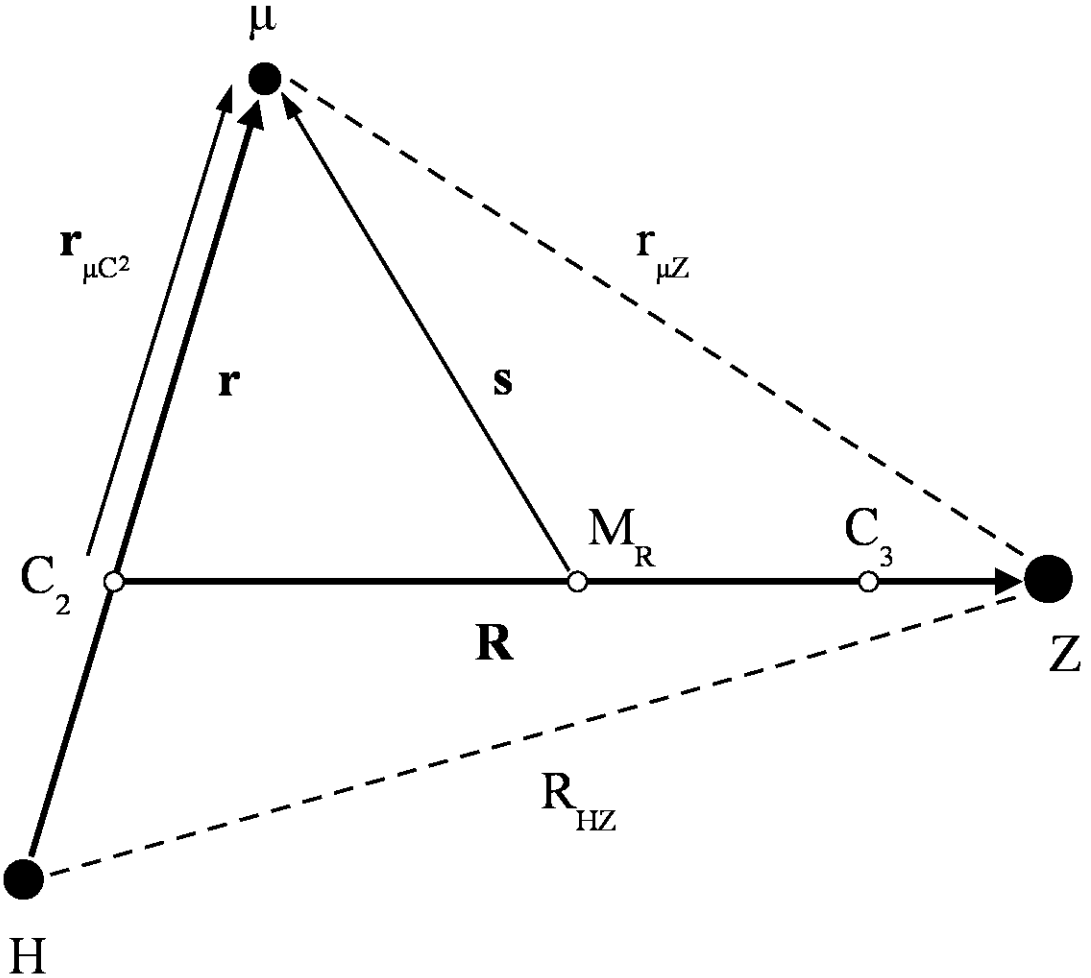


Figure 1: The Jacobi coordinates of the entrance channel and other notations. C_2 is the centre of mass of muonic hydrogen, C_3 is the centre of mass of the three-body system, M_R is the midpoint of the vector \mathbf{R} .

Let us isolate a two-centre problem in the three-body Hamiltonian. For this purpose the term \hat{H}_μ is rewritten as follows [14]:

$$\hat{H}_\mu = m_{\mu H} \cdot \hat{h}_\mu, \quad (7)$$

$$\hat{h}_\mu = -\frac{1}{2} \Delta_s - \frac{1}{|\mathbf{s} + \frac{\mathbf{R}}{2}|} - \frac{Z'}{|\mathbf{s} - \frac{\mathbf{R}}{2}|}. \quad (8)$$

The vector \mathbf{s} connects the midpoint M_R of the vector \mathbf{R} with the muon (Fig. 1):

$$\mathbf{s} = \mathbf{r}_{\mu C_2} - \frac{\mathbf{R}}{2}, \quad \mathbf{r}_{\mu C_2} = m_{\mu H} \cdot \mathbf{r}. \quad (9)$$

The vector $\mathbf{r}_{\mu C_2}$ joins the centre of mass of muonic hydrogen and the muon. The quantity Z' is:

$$Z' = \frac{Z}{m_{\mu H}}. \quad (10)$$

\hat{h}_μ is the Hamiltonian of the muon in the field of two Coulomb centres whose charges are equal to unity and Z' . The unit charge is placed in the centre of mass of muonic hydrogen, the position of the charge Z' coincides with the one of the nucleus Z . For the muon transfer from protium to neon

$$m_{\mu H} \approx 0.899, \quad Z' \approx 11.1. \quad (11)$$

In the coordinate frame with the origin in the point M_R and the polar axis directed along the vector \mathbf{R} , the position of the muon is specified by prolate spheroidal coordinates ξ , η and φ [15]:

$$\xi = \frac{r_{\mu C_2} + r_{\mu Z}}{R}, \quad \eta = \frac{r_{\mu C_2} - r_{\mu Z}}{R}, \quad (12)$$

R is the length of the vector \mathbf{R} . The azimuthal angle φ lies in the plane passing through the point M_R perpendicularly to \mathbf{R} . Surfaces of constant values of the coordinates ξ and η are prolate ellipsoids of revolution and two-sheeted hyperboloids with the focuses in the points C_2 and Z . For these points $\xi = 1$ and $\eta = \mp 1$.

Let us consider the eigenvalue and eigenfunction problem for the two-centre Hamiltonian \hat{h}_μ :

$$\hat{h}_\mu \psi_{jm}(\xi, \eta; R) \frac{\exp(\pm im\varphi)}{\sqrt{2\pi}} = \varepsilon_{jm}(R) \psi_{jm}(\xi, \eta; R) \frac{\exp(\pm im\varphi)}{\sqrt{2\pi}}. \quad (13)$$

The dependence on the angle φ is explicitly indicated here, m is a nonnegative integer, the subscript j denotes a set of the other quantum numbers. For bound states these are either the numbers n_ξ and n_η of nodes in the corresponding variables or the parabolic quantum numbers n_1 and n_2 in the limit $R \rightarrow \infty$ [15]. The two-centre problem (13) is solved at a fixed distance R which appears in eigenfunctions and eigenvalues as a parameter. The eigenfunctions with the same m and different sets i and j of the other quantum numbers are orthonormal:

$$\int \psi_{im}(\xi, \eta; R) \psi_{jm}(\xi, \eta; R) d\tau = \delta_{ij}; \\ d\tau = (R/2)^3 (\xi^2 - \eta^2) d\xi d\eta. \quad (14)$$

The integral is taken over the region $1 \leq \xi < \infty$, $-1 \leq \eta \leq +1$. The orthonormalization with respect to m is provided by the factors $\exp(\pm im\varphi)/\sqrt{2\pi}$. It is obvious that the solutions of the problem (13) are the eigenfunctions of the Hamiltonian \hat{H}_μ with the eigenvalues $m_{\mu H} \cdot \varepsilon_{jm}(R)$.

It is well known that the two-centre problem permits separation of variables in the prolate spheroidal coordinates [15]. Every eigenfunction $\psi_{jm}(\xi, \eta; R)$ is the product of radial and angular

functions depending separately on ξ and η . Solving a pair of differential equations for these functions under suitable boundary conditions allows one to find the eigenvalue $\varepsilon_{jm}(R)$ and the separation constant and, finally, to construct the functions. In ref. [5] this procedure was realized on the basis of comparison equations suggested in ref. [16]. The method of solving the two-centre problem was improved in the present work. Namely, an algorithm based on the well-known infinite expansions [17–19] of the radial and angular functions was implemented in practice. The eigenvalue $\varepsilon_{jm}(R)$ and the separation constant were determined according to the method suggested in ref. [20] and modified for the case in which expansion coefficients are nonmonotonic functions of their number.

The three-body system is considered in an initial coordinate frame with fixed axes and the origin in the centre of mass C_3 . Let us introduce the operator $\hat{\mathbf{J}}$ of the orbital angular momentum of the three-body system. The Hamiltonian \hat{H} commutes with the operator $\hat{\mathbf{J}}^2$ of its square and with the operator \hat{J}_z of its projection on the z -axis of the initial frame. Moreover, \hat{H} commutes with the operator \hat{P} of the coordinate inversion. A convenient basis in which the three-body wavefunction is expanded consists of eigenfunctions of these three operators. Let us require them to be eigenfunctions of the two-centre problem (13). As the spheroidal coordinates of the muon are defined with respect to the vector \mathbf{R} , let us introduce the polar angle Θ and the azimuthal angle Φ specifying the direction of \mathbf{R} in the initial coordinate frame. Then a configuration of the three-body system is specified by the independent variables $R, \Theta, \Phi, \xi, \eta, \varphi$; and the basis functions are:

$$\Psi_{Mjm}^{JP}(R, \Theta, \Phi, \xi, \eta, \varphi) = \frac{\chi_{jm}^{JP}(R)}{R} \Upsilon_{Mm}^{JP}(\Phi, \Theta, \varphi) \psi_{jm}(\xi, \eta; R). \quad (15)$$

$\chi_{jm}^{JP}(R)$ is a radial function depending on the indicated quantum numbers, $\Upsilon_{Mm}^{JP}(\Phi, \Theta, \varphi)$ is the eigenfunction of the operators $\hat{\mathbf{J}}^2$, \hat{J}_z , and \hat{P} with the eigenvalues $J(J+1)$, M , and P . The nonnegative integer m introduced in (13) is the modulus of the projection of the angular momentum on the direction of the vector \mathbf{R} . The functions Υ_{Mm}^{JP} are orthonormal:

$$\int_0^\pi \sin \Theta d\Theta \int_0^{2\pi} d\Phi \int_0^{2\pi} d\varphi (\Upsilon_{Mm}^{JP})^* \Upsilon_{M'm'}^{J'P'} = \delta_{JJ'} \delta_{PP'} \delta_{MM'} \delta_{mm'}. \quad (16)$$

Their form depends on m . If $m = 0$, then

$$\Upsilon_{Mm=0}^{JP}(\Phi, \Theta, \varphi) = \frac{Y_{JM}(\Theta, \Phi)}{\sqrt{2\pi}}, \quad (17)$$

$Y_{JM}(\Theta, \Phi)$ is the ordinary spherical function. In this case the parity is unambiguously specified by the quantum number J : $P = (-1)^J$. If $m \neq 0$, then

$$\Upsilon_{Mm}^{JP}(\Phi, \Theta, \varphi) = \frac{\sqrt{2J+1}}{4\pi} \left[(-1)^m D_{Mm}^J(\Phi, \Theta, \varphi) + P(-1)^J D_{M(-m)}^J(\Phi, \Theta, \varphi) \right], \quad (18)$$

D_{Mm}^J and $D_{M(-m)}^J$ are the Wigner functions [21] transformed under the inversion as follows:

$$D_{Mm}^J(\Phi, \Theta, \varphi) \longrightarrow (-1)^{J-m} D_{M(-m)}^J(\Phi, \Theta, \varphi). \quad (19)$$

In this case the two values of the parity are possible at given J : $P = \pm(-1)^J$.

Let us consider the time-independent Schrödinger equation for the three-body wavefunction with the quantum numbers J , M , and P :

$$\hat{H} \Psi_M^{JP} = E \Psi_M^{JP}. \quad (20)$$

For the reaction (1) the energy is:

$$E = E_{\mu\text{H}}(1S) + E_c. \quad (21)$$

$E_{\mu\text{H}}(1S)$ is the energy of the ground state of muonic hydrogen:

$$E_{\mu\text{H}}(1S) = -\frac{m_{\mu\text{H}}}{2}, \quad (22)$$

E_c is the collision energy:

$$E_c = \frac{M_r v^2}{2} = \frac{k^2}{2M_r}, \quad (23)$$

v is the velocity of the relative motion of the μH atom and the nucleus Z at infinite separation, $k = M_r v$ is the asymptotic momentum of the relative motion.

Let us seek a solution of the Schrödinger equation in the form of an expansion in the basis functions (15):

$$\Psi_M^{JP} = \sum_{jm} \Psi_{Mjm}^{JP}. \quad (24)$$

The substitution of this expansion into the equation (20) and the integration over the variables Θ , Φ , ξ , η , and φ under the orthonormalization condition (16) yield a set of coupled second-order differential equations for the radial functions $\chi_{jm}^{JP}(R)$. These equations are given in ref. [5]. In practice, a finite number of two-centre states is taken into account in the expansion (24). Solving the obtained set of coupled equations under suitable boundary conditions allows one to calculate the total cross-section of the reaction (1).

As already noted, the main idea of the present approach is to provide the asymptotically correct description of the entrance channel of the muon transfer reaction at large distances R . In the limit $R \rightarrow \infty$ the bound eigenstates of the two-center problem (13) fall into two groups. The states of one group are localized near the left centre, which is placed in the centre-of-mass of the μH atom and has the unit charge. The states of another group are localized near the right centre Z' . The simplest way to describe the entrance channel is to take into account the only state of the left-centre group. Its asymptotic quantum numbers are:

$$m = n_1 = n_2 = 0, \quad n = 1. \quad (25)$$

n_1 and n_2 are the parabolic quantum numbers [15], $n = n_1 + n_2 + m + 1$ is the principle quantum number. All the quantities related to this state will be marked with the subscript 0. In the limit considered, the eigenfunction ψ_0 and the eigenvalue $\varepsilon_0(R)$ of the two-centre problem are:

$$\psi_0 \propto \exp(-m_{\mu\text{H}} \cdot r), \quad \varepsilon_0(R \rightarrow \infty) = -\frac{1}{2}. \quad (26)$$

Thus, the two-centre eigenfunction goes into the wavefunction of the ground state of muonic hydrogen with the correct reduced mass. This is due to the left centre being placed in the centre-of-mass of muonic hydrogen. The argument of the exponent in the function ψ_0 is the distance from this centre to the muon. The eigenvalue of the Hamiltonian \hat{H}_μ tends to the correct dissociation limit:

$$m_{\mu\text{H}} \cdot \varepsilon_0(R \rightarrow \infty) = E_{\mu\text{H}}(1S). \quad (27)$$

At large R the relative motion in the entrance channel is governed by the potential $U_0(R)$ which is a result of averaging the three-body Hamiltonian over the state ψ_0 . The expansion of this potential in powers of R^{-1} was considered in ref. [5]. Its leading term is proportional to R^{-4} and corresponds to the polarization attraction of muonic hydrogen and the nucleus Z :

$$U_0(R) = -\frac{\beta_0 Z^2}{2R^4}. \quad (28)$$

The following value was obtained for the dipolar polarizability of muonic hydrogen:

$$\beta_0 = \beta \left[1 - \frac{1}{(M_{\text{H}} + 1)^2} \right], \quad (29)$$

β is the exact value of the polarizability:

$$\beta = \frac{9}{2m_{\mu\text{H}}^3}. \quad (30)$$

It should be noted that, because of the cube of the reduced mass in the denominator of this formula, the value of β may differ noticeably from the frequently used value of 4.5, which corresponds to an infinitely heavy nucleus H. In particular, $\beta \approx 6.20$ for muonic protium. Although β_0 is not equal to β , their values are very close. For muonic protium $\beta_0 \approx 0.99\beta$. The difference of these values is due to the Coulomb repulsion of the nuclei being nondiagonal in the two-centre basis. It was shown in ref. [5] that taking into account this fact yielded a small correction whose addition to β_0 faithfully reproduces the polarizability β . Thus, the use of the only left-centre state already provides a good description of the entrance channel at large R : the dissociation limit is correct, no spurious long-range interactions appear (at least in the terms up to R^{-4} inclusive), the polarizability of muonic hydrogen is reproduced with one percent accuracy. Therefore, this description will be followed below. In addition, as the values of β and β_0 agree closely with each other, the polarization potential with the exact value of β will be used to describe the relative motion in the entrance channel at large R :

$$U_p(R) = -\frac{\beta Z^2}{2R^4}. \quad (31)$$

In the approach considered, the muon transfer channel is described by right-centre states. In the limit $R \rightarrow \infty$ they correspond to the $\mu Z'$ atom with an infinitely heavy nucleus, but not to the real μZ atom. In particular, the wavefunctions of these states do not include the reduced mass of the μZ atom at all. Moreover, the equations for the radial functions of the transfer channel remain

coupled at $R \rightarrow \infty$, although, as it was found in ref. [5], coupling matrix elements are not too large compared to the energy released in the transfer reaction. The reason of these difficulties lies in the transfer channel being described in the Jacobi coordinates of the entrance channel. It is obvious that no partial transfer cross-sections to individual states of the μZ atom can be calculated in this case. Nevertheless, as at large R the right-centre states are localized near the nucleus Z , whose position coincides with the one of the charge Z' , a group of these states as a whole describes the migration of the muon charge cloud from H to Z , i.e. the muon transfer. Therefore, it is possible to calculate the total transfer cross-section. Let us consider how this is done.

The matrix elements of the three-body Hamiltonian coupling the entrance and transfer channels fall exponentially at large R . Therefore, in the limit $R \rightarrow \infty$ the set of radial equations is split into two blocks which correspond to the entrance and transfer channels. In the simplest approximation in which the only left-centre state with the quantum numbers (25) is taken into account, the entrance channel is described by one equation:

$$\frac{d^2\chi_0^J}{dR^2} + \left[k^2 - \frac{J(J+1)}{R^2} - 2M_r U_p(R) \right] \chi_0^J = 0. \quad (32)$$

χ_0^J is the radial function of the entrance channel. Its superscript P is omitted because the parity is now specified by the quantum number J : $P = (-1)^J$. The boundary condition at large R is:

$$\chi_0^J(R \rightarrow \infty) \rightarrow \sin(kR - J\pi/2) + Q_0^J \exp[i(kR - J\pi/2)]. \quad (33)$$

The complex amplitude Q_0^J depends on J and k . The radial functions of the transfer channel are asymptotically represented by outgoing scattered waves. A method of constructing such solutions for coupled equations was described in ref. [5]. The boundary condition at $R = 0$ is standard: all the radial functions are equal to zero in this point.

The integration of coupled equations under the above boundary conditions allows one to construct the amplitudes Q_0^J . Let us rewrite the asymptotic radial function χ_0^J in the following form:

$$\chi_0^J(R \rightarrow \infty) \rightarrow \frac{i}{2} \left[\exp\left(-kR + \frac{J\pi}{2}\right) - S_0^J \exp\left(kR - \frac{J\pi}{2}\right) \right]. \quad (34)$$

S_0^J is the diagonal S -matrix element corresponding to the entrance channel:

$$S_0^J = 1 + 2i Q_0^J. \quad (35)$$

As the muon transfer is the only inelastic channel at the collision energies considered, the total transfer cross-section is [21]:

$$\sigma(E_c) = \frac{\pi}{k^2} \sum_{J=0}^{\infty} (2J+1) \left(1 - |S_0^J|^2 \right). \quad (36)$$

The muon transfer rate treated as a function of the collision energy and reduced to the atomic density of liquid hydrogen is:

$$q(E_c) = N_{\text{H}} v \sigma(E_c). \quad (37)$$

The transfer rate $\lambda(T)$ from thermalized μH atoms is obtained by averaging this quantity over the Maxwellian distribution of relative velocities in the entrance channel.

3. SOME DETAILS OF THE CALCULATIONS

Let us consider how the method described in Section 2 is applied to the calculation of the rate of the muon transfer from protium to neon. At large interatomic separations, the entrance channel is described by the only left-centre state ψ_0 with the quantum numbers (25). In order to choose the relevant right-centre states, let us take advantage of the standard viewpoint that the muon transfer from hydrogen to a heavier nucleus is mainly due to quasicrossings of adiabatic terms associated with the reaction channels. Let us specify the right-centre states by the parabolic quantum numbers n'_1 , n'_2 , and the principle quantum number $n' = n'_1 + n'_2 + m + 1$. It is known [15] that the quasicrossings occur for terms with the same quantum numbers m and n_1 . As the state ψ_0 has the zeroth values of these numbers, let us confine ourselves to right-centre states with $m = n'_1 = 0$. Their wavefunctions have no nodes in the variable ξ , but differ in the number n_η of nodes in the variable η . The states with $5 \leq n'_2 \leq 10$ will be of interest in the following discussion. According to the relations between n_η and n'_2 presented in the treatise [15], for these states $n_\eta = n'_2$ at $Z' \approx 11.1$. The dependences of the eigenvalues ε_j of the two-centre problem (13) on the interatomic distance R are shown in Figure 2 for the states with $n'_2 = 5-8$; the subscript j is now reduced to the parabolic quantum number n'_2 . There are quasicrossings at $R \approx 8, 13$, and 21. As R is increased, the value of n'_2 increases by unity at each quasicrossing. This corresponds to the general rule [15] that the terms involved into a quasicrossing differ in the number n_η by unity. There are three more quasicrossings not shown in Figure 2. Two of them lie at $R \approx 37$ and 85. In passing through each of these quasicrossings in the direction of growth of R , the number n'_2 increases by unity and takes on the values of 9 and 10. Finally, the outermost quasicrossing lies at $R \approx 878$. It involves the right-centre state with $n'_2 = 10$ and the state ψ_0 for which the number of nodes $n_\eta = 11$.

Let us assume that muonic protium and neon are separated by a very large distance R . The function ψ_0 corresponding to this case is localized near the proton and practically identical there to the atomic $1S$ -state wavefunction. All their eleven nodes are located near the neon nucleus where ψ_0 is exponentially small. Such a situation survives to the outermost quasicrossing with the right-centre state for which $n'_2 = 10$. After passing a very narrow quasicrossing region, the muon charge distribution in these states changes drastically. In the state ψ_0 the muon charge cloud migrates to neon and becomes exponentially small near the proton. In the state with $n'_2 = 10$ everything is opposite: the charge flows to the proton and all the nodes of the wavefunction prove in a region near neon where the wavefunction is exponentially small. A similar situation is observed in passing through the other long-distance quasicrossings which occur deep under the potential barrier separating the Coulomb wells of the two-centre problem. Therefore, it is valid to say that between narrow quasicrossing regions the muon charge cloud is localized near one of the Coulomb centres and, as R is reduced, the right-centre states with the number n'_2 decreasing in successive unit steps describe muonic protium in the Coulomb field of neon. In particular, in the interval $21 < R < 37$ this is the state with $n'_2 = 8$. The fact that it corresponds to muonic protium in the

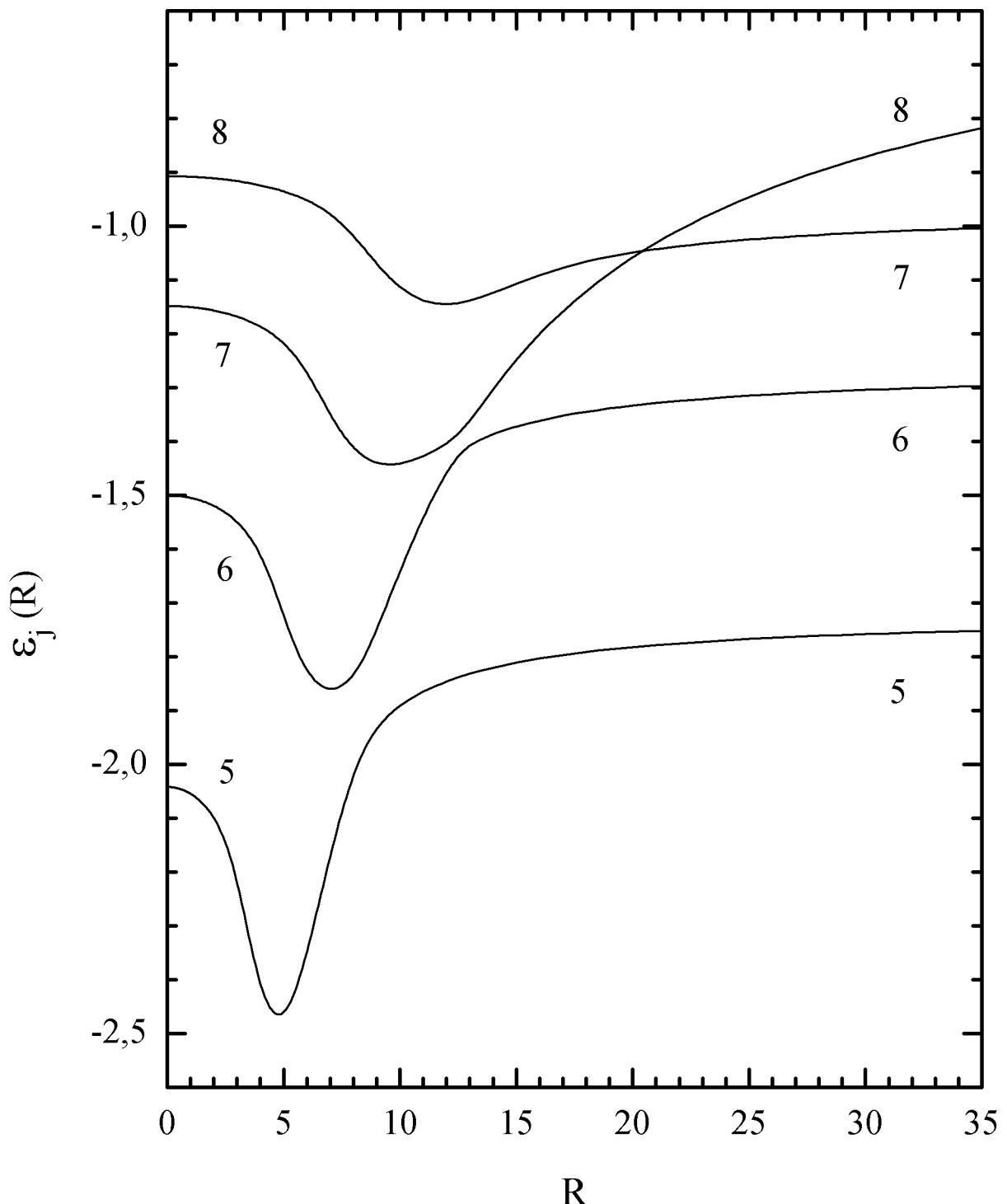


Figure 2: The eigenvalues $\varepsilon_j(R)$ of the two-centre Coulomb problem vs. the interatomic distance R for the right-centre states with the parabolic quantum numbers $m = n'_1 = 0$ and $n'_2 = 5 - 8$. All the quantities are given in m.a.u. The curves are marked with values of the number n'_2 .

field of neon is confirmed by calculations of the adiabatic potential which is equal to the sum of the eigenvalue $m_{\mu H} \cdot \varepsilon_j(R)$ of the Hamiltonian \hat{H}_μ and the mean value of the Coulomb repulsion of the nuclei. At $R \sim 30$ this potential agrees with the polarization potential $U_p(R)$ with one percent accuracy. With further decrease in R the quasicrossings occur nearer and yet nearer to the barrier top, the quasicrossing regions become broader, and the statement on the muon localization near one of the nuclei loses its meaning. For example, the quasicrossing at $R \approx 8$ occurs near the barrier top.

According to the standard viewpoint, the muon transfer is due to not too distant quasicrossings occurring near the barrier top. For example, the muon transfer to carbon and oxygen results from quasicrossings at $R = 7 - 9$ [4], the transfer to fluorine is due to the ones at $R \approx 12$ [22]. In ref. [3] the transfer to neon was attributed to quasicrossings at $R \approx 26$. Therefore, in the present work only the four right-centre states with the quantum numbers $m = n'_1 = 0$ and $n'_2 = 5 - 8$ were taken into account in the expansion of the three-body wavefunction (Fig. 2). In this case there is a set of four coupled radial equations in the region lying on the left of the quasicrossing at $R \approx 21$. On the right of this quasicrossing, the state with $n'_2 = 8$ describes muonic protium in the field of neon. The matrix elements coupling the equation for the radial function of this state with the other equations fall exponentially in increasing R . Therefore, at $R \sim 30$ this equation is separated from the others and corresponds to the entrance channel of the transfer reaction. As it was already mentioned, at this value of R the adiabatic potential in this equation agrees with the polarization potential with one percent accuracy. At $R > 30$ the equation (32) with the polarization potential $U_p(R)$ was used for the description of the entrance channel, i.e. all the deep subbarrier quasicrossings lying at $R \geq 37$ were fully ignored. In this case the transfer channel is described by the three radial equations for the states with $n'_2 = 5 - 7$.

The above consideration related to the muon transfer to a bare nucleus Z . Actually, muonic hydrogen collides with an atom or a molecule which have an electron shell. The energy gain in the transfer reaction is a few keV, and it is more than enough for an electron excitation. An analysis of the dynamics of the electron shell during the collision is a complicated problem including a construction of electron terms in the Coulomb field of the three-body system μHZ and an examination of transitions between them. The simplest approximation is to ignore any excitations and to assume that the electron shell remains in its ground state during the collision. In this case the role of the electron shell is reduced to the screening of the Coulomb interaction of heavy particles in the reaction channels. It is natural to expect that because of small collision energies the screening is most significant in the entrance channel. In the present work the screening was taken into account in the equation (32) which describes the entrance channel at $R > 30$. Instead of the polarization potential $U_p(R)$, a new potential $U_e(R)$ was used in this equation. The method of its construction was suggested in ref. [23]. For the interaction of muonic hydrogen with a noble gas atom at collision energies below the lowest excitation energy of the electron shell (16.6 eV for neon), the potential $U_e(R)$ is:

$$U_e(R) = U_s(R) + U_f(R) + U_w(R). \quad (38)$$

The first term is the screened polarization potential:

$$U_s(R) = -\frac{\beta Z_a^2(R)}{2R^4}, \quad Z_a(R) = Z - Z_e(R). \quad (39)$$

$Z_e(R)$ is the absolute value of the electron charge inside the sphere of the radius R centered at the nucleus Z , $Z_a(R)$ is the total atomic charge in this sphere. The term $U_f(R)$ may be treated as a contact interaction of muonic hydrogen with the electron shell:

$$U_f(R) = \frac{2\pi}{3} \langle r_{\mu H}^2 \rangle \rho_e(R). \quad (40)$$

$\langle r_{\mu H}^2 \rangle$ is the mean-square charge radius of muonic hydrogen in the $1S$ -state. It is calculated with respect to the centre of mass of μH :

$$\langle r_{\mu H}^2 \rangle = -\frac{3}{m_{\mu H}} \left(1 - \frac{1}{M_H} \right). \quad (41)$$

This quantity is negative because it is mainly contributed by the negatively charged muon. The function $\rho_e(R)$ is the absolute value of the electron density at the distance R from the nucleus Z . It is normalized as follows:

$$4\pi \int_0^\infty \rho_e(R) R^2 dR = Z. \quad (42)$$

The charge $Z_e(R)$ and the density $\rho_e(R)$ were calculated with analytical one-electron wavefunctions obtained within the Roothan-Hartree-Fock method [24]. Both the potentials $U_s(R)$ and $U_f(R)$ are attractive and fall exponentially with increasing R . As $U_s(R)$ is proportional to the square of $Z_a(R)$ and, in addition, to R^{-4} , it falls faster. As a result, this potential is significant at distances R less than the electron Bohr radius (≈ 200 m.a.u.). For example, at $R = 30$ the potential $U_s \approx -1.7$ eV and it exceeds U_f by an order of magnitude. As the electron K -shell of neon is similar in size, the screening effect on the potential U_s is already noticeable: the charge $Z_a \approx 8.9$. At $R \approx 100$ the potentials U_s and U_f become equal to each other and their sum is about -0.02 eV, i.e. it is of the order of thermal energies at room temperature. At $R \approx 200$ the term U_s is already about 5% of U_f . The latter is equal to -0.002 eV.

The last term $U_w(R)$ in the formula (38) appears in the second order of the perturbation theory with respect to the Coulomb interaction of atomic electrons with muonic hydrogen. It corresponds to the van der Waals attraction at large R . An accurate calculation of this potential is not a simple matter because it involves the summation over intermediate states of both the electron shell and muonic hydrogen. The asymptotic expansion of this potential in powers of R^{-1} was considered in ref. [5]. Its leading term has the standard form $(-C/R^6)$. The constant C was estimated in the completeness approximation: $C = 1.90 \times 10^{+6}$ m.a.u. In this case the potential $U_e(R)$ was written in the simplest form which provides the correct asymptotic behaviour at large R :

$$U_e(R) = \begin{cases} U_s(R) + U_f(R) & , R < R_w; \\ -C/R^6 & , R \geq R_w. \end{cases} \quad (43)$$

Table 2: The position R_b of the top of the effective-potential barrier and its height U_b for some angular momenta J in the cases A–C. In each box the upper value is R_b in m.a.u., the lower value is U_b in eV.

J	A	B	C
1	76.1 0.0519	62.4 0.0841	65.6 0.0672
2	44.0 0.467	39.0 0.641	40.5 0.577
3	31.1 1.87	28.9 2.32	29.5 2.17

R_w is the interatomic separation at which the sum $U_s(R) + U_f(R)$ becomes equal to the van der Waals potential $(-C/R^6)$. For neon $R_w \approx 1070$ m.a.u. (≈ 2.7 Å) and the potential at this distance is very small: $U_e(R_w) \approx 7 \times 10^{-9}$ eV. Therefore, the van der Waals tail of the potential is insignificant at the considered collision energies $E_c \geq 10^{-4}$ eV, and it is possible to set $U_e(R) = U_s(R) + U_f(R)$ for all R .

In order to clarify the role of the electron screening, the calculations were made for the same cases A, B, and C as in ref. [5] (Sect. 1). These cases differ in the potential in the equation (32) asymptotically describing the entrance channel. The unscreened polarization potential $U_p(R)$ was used in the case A. This corresponds to the muon transfer to the bare neon nucleus. The screened potential $U_s(R)$ was substituted for $U_p(R)$ in the case B, and the potential $U_e(R) = U_s(R) + U_f(R)$ was employed in the case C. In all these cases, for nonzero angular momenta J there is a barrier in the effective potential appearing in the equation (32). The position R_b of the barrier top and its height U_b are given in Table 2 for $J \leq 3$. For these values of J the barrier top lies in the region $R > 30$ in which the entrance channel is described by the equation (32). It is interesting that the weakening of the attraction caused by the electron screening leads to the barrier top being shifted to lower R and its height increasing. This fact was pointed out in ref. [13]. At low collision energies $E_c \ll U_b$, the barrier prevents the penetration of the corresponding partial wave into the interaction region. As a result, the contribution of this wave to the transfer cross-section is small. As the collision energy goes up to the barrier top, the partial transfer cross-section increases and becomes comparable to contributions of waves with lower angular momenta. Moreover, quasi-steady states may exist under the barrier. The transfer cross-section has a resonance peak in a vicinity of such a state. In ref. [5] one quasi-steady state was found in the D -wave at collision energies of 0.3–0.5 eV.

4. RESULTS OF THE CALCULATIONS AND CONCLUSIONS

The energy dependences of the transfer rate $q(E_c)$ are shown in Figure 3. They are similar to those found in ref. [5]. At low collision energies, the S -wave makes the main contribution, the cross-section is proportional to v^{-1} , and the transfer rate is nearly constant. Its values depend on

the way of taking into account the electron screening, but in a less degree than in ref. [5]. With a rise in the collision energy, the transfer rate obtained in the cases A and C decreases, while in the case B it remains almost constant. The contribution of the P -wave becomes significant at energies corresponding to room temperature, and the transfer rate begins to go up gradually. As a result, in the cases A and C there is a broad minimum covering the region of thermal energies. This corresponds qualitatively to the strong suppression of the transfer reaction at room temperature. On the whole, at $E_c < 0.1$ eV the curves of $q(E_c)$ found in the present work are obtained by moving the curves of ref. [5] down. With further increase in the collision energy, the D -wave begins to play a dominant role. In all the cases A–C, there is a resonance peak on the curve $q(E_c)$ at $E_c \approx 0.5$ eV. It is due to the already mentioned quasi-steady state in the D -wave. Parameters of this peak, such as its position, width, and height, depend slightly on the electron screening. It is interesting that in ref. [5] the resonance peak was obtained only in the cases B and C, and its parameters were more sensitive to the electron screening. Moreover, compared to the present work the peak was noticeably higher and wider. The effect of the D -wave resonance is manifested up to the energy $E_c \approx 2$ eV. Then the transfer rate passes through one more minimum, and at $E_c > 5$ eV it begins to go up again due to the contribution of waves with $J \geq 3$. The electron screening is already insignificant in this region, and the curves obtained in the cases A–C are practically identical. It should be noted that the rapid increase of the muon transfer rate at $E_c > 0.2$ eV is of interest in connection with the question of a measurement of the hyperfine splitting of the $1S$ -state of muonic protium [11].

The temperature dependences of the rate $\lambda(T)$ of the muon transfer from thermalized μp atoms are shown in Figure 4. They were obtained by averaging $q(E_c)$ over the Maxwellian distribution of relative velocities in the entrance channel. The values of $\lambda(T)$ at the temperatures of 20 K and 300 K are given in the last column of Table 1. The curves obtained in the present work lie below the corresponding curves of ref. [5]. The curve found in the most realistic case C correctly reproduces the tendency to decreasing the transfer rate with increasing the temperature in the interval 20–300 K. At $T = 20$ K it passes through the lowest point of the interval of experimental values. At $T = 300$ K the calculated value of $\lambda(T)$ exceeds the experimental value by a factor of 1.5. The curve obtained in the case A lies at greater values of the transfer rate, and it is nearly parallel to the curve C. The value of $\lambda(T)$ found in the case B for room temperature agrees very well with the experiment (the accuracy is about 2 %), but at lower temperatures the transfer rate is nearly constant. At high temperatures the values of $\lambda(T)$ obtained in the case C go up more slowly than in ref. [5]. This is due to the shift of the resonance peak on the curve of $q(E_c)$ to greater energies and the decrease of its width and height. On the whole, the results obtained in the present work agree with the experimental data better than the results of ref. [5]. The effect of the electron screening proves to be somewhat less, but still noticeable.

This work was supported by the Grant NS–215.2012.2 from the Ministry of Education and Science of the Russian Federation.

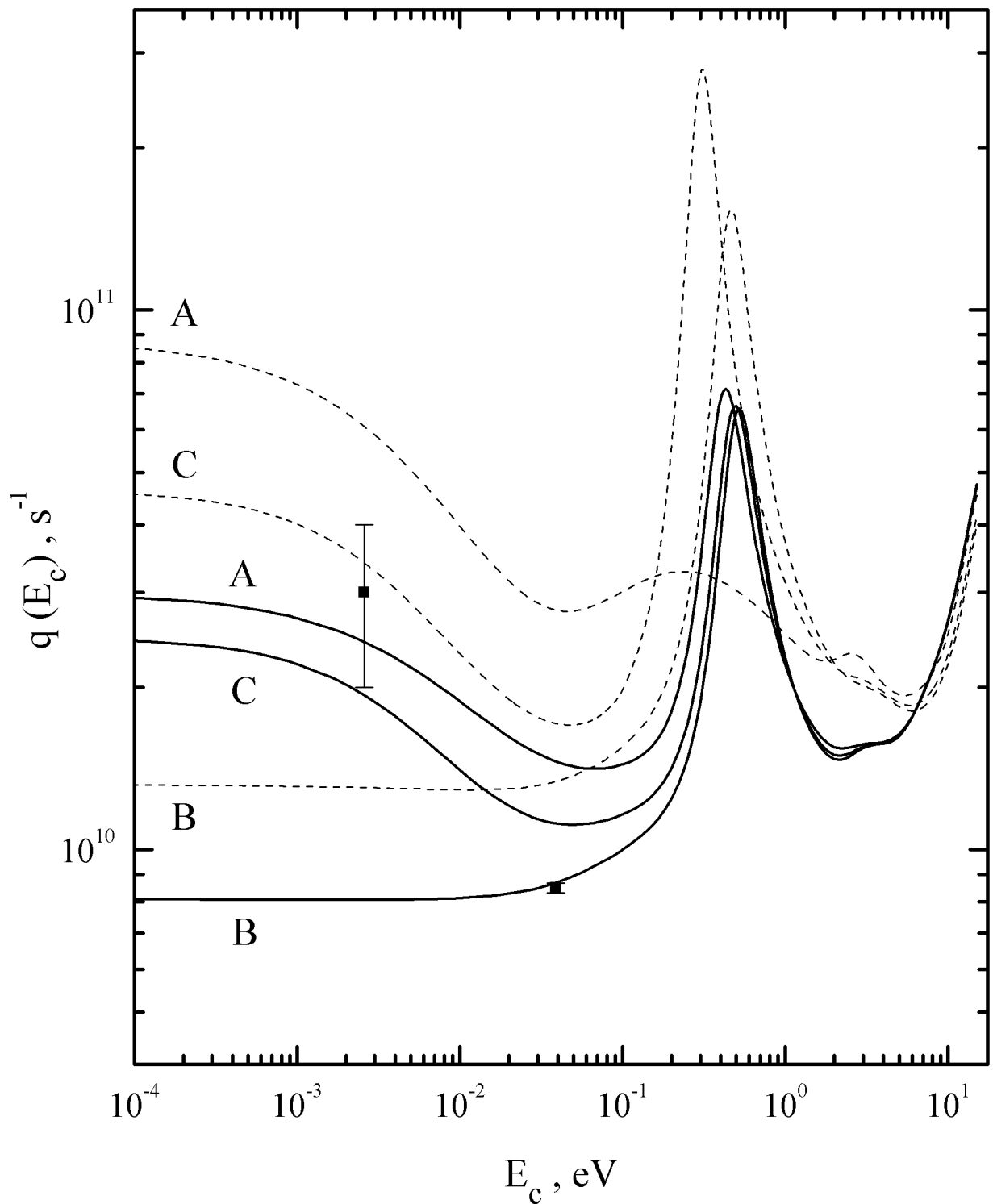


Figure 3: The muon transfer rate $q(E_c)$ vs. the collision energy E_c . The rate is reduced to the atomic density of liquid hydrogen. The solid curves are the results of the present work, the dashed curves are the results obtained in ref. [5]. The curves are marked with the letters A, B, and C in accordance with the three ways of taking into account the electron screening. The experimental values of the transfer rate (Table 1) are attributed to the mean thermal energies $(3/2)kT$ at $T = 20$ and 300 K.

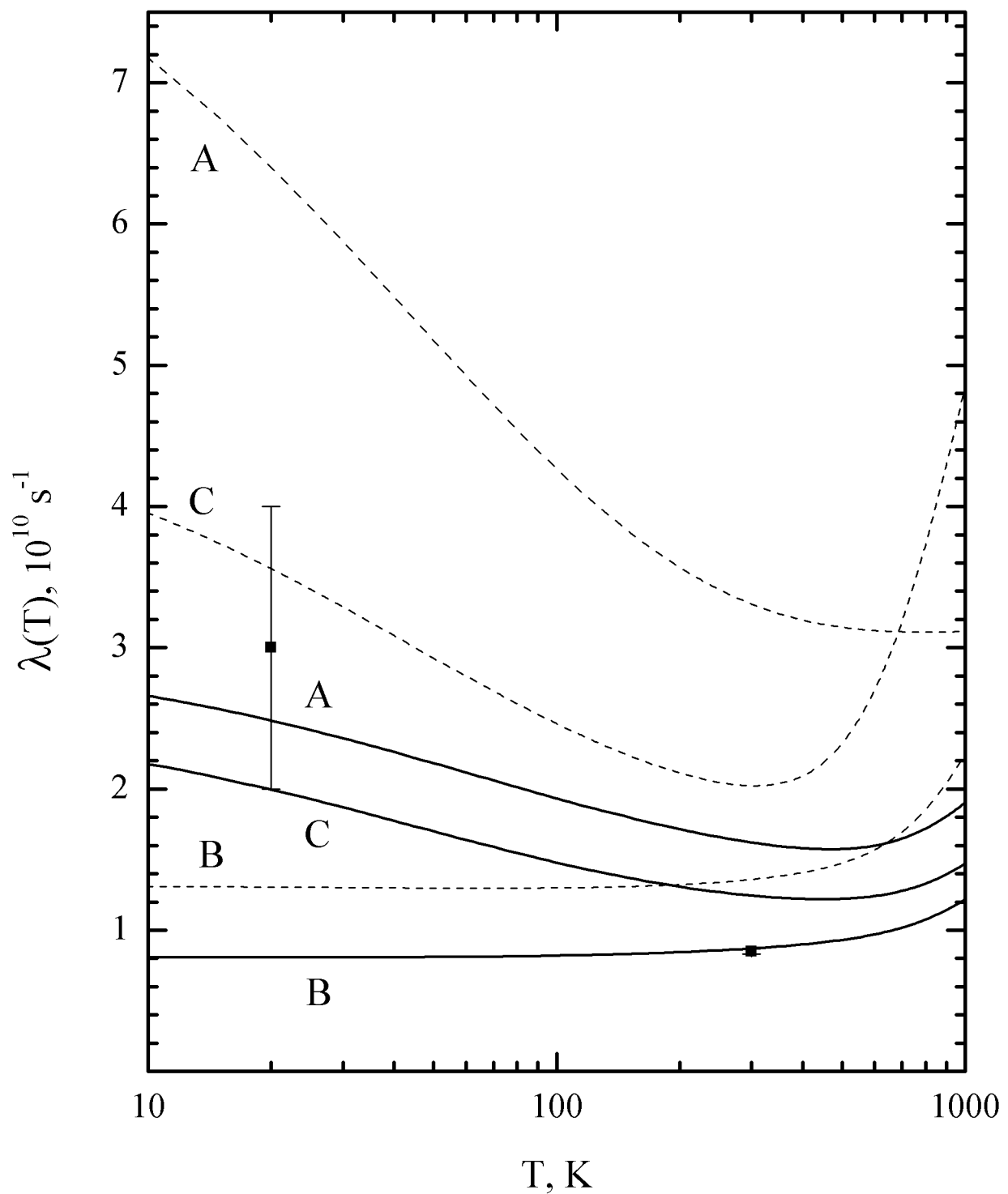


Figure 4: The rate $\lambda(T)$ of the muon transfer from thermalized μp atoms vs. the temperature T . The rate is reduced to the atomic density of liquid hydrogen. The notations of the curves are identical to those used in Figure 3. The experimental values correspond to the temperatures $T = 20$ and 300 K (Table 1).

-
- [1] L. Schellenberg, Muon Cat. Fusion **5/6**, 73 (1990/91) and references therein.
- [2] R. Jacot-Guillarmod, Phys. Rev. **A51**, 2179 (1995).
- [3] Yu. S. Sayasov, Helv. Phys. Acta **63**, 547 (1990).
- [4] S. S. Gershtein, Sov. Phys. JETP **16**, 501 (1963).
- [5] S. V. Romanov, Eur. Phys. J. **D28**, 11 (2004).
- [6] R. Pohl *et al.*, Nature **466**, 213 (2010).
- [7] D. Taqqu, preprint PSI-PR-95-07 (Paul Scherrer Institute, Villigen, 1995).
- [8] R. Pohl *et al.*, Hyperf. Interact. **119**, 77 (1999).
- [9] A. A. Radzig and B. M. Smirnov, *Parameters of Atoms and Atomic Ions* (Energoatomizdat, Moscow, 1986), Sect. 6.1 (*in Russian*).
- [10] S. I. Vinitskii and L. I. Ponomarev, Sov. J. Part. Nucl. **13**, 557 (1982).
- [11] A. Dupays, B. Lepetit, J. A. Beswick, C. Rizzo, and D. Bakalov, Phys. Rev. **A69**, 062501 (2004).
- [12] A. Dupays, Phys. Rev. Lett. **93**, 043401 (2004).
- [13] G. Fiorentini and G. Torelli, Nuovo Cim. **A36**, 317 (1976).
- [14] K. Kobayashi, T. Ishihara, and N. Toshima, Muon Cat. Fusion **2**, 191 (1988).
- [15] V. I. Komarov, L. I. Ponomarev, and S. Yu. Slavyanov, *Spheroidal and Coulomb Spheroidal Functions* (Science Publ., Moscow, 1976), Chap. 2, Sects. 3.1–3.3, 3.5 (*in Russian*).
- [16] D. A. Abramov, S. Yu. Ovchinnikov, and E. A. Solov'ev, Phys. Rev. **A42**, 6366 (1990).
- [17] G. Jaffé, Z. Phys. **87**, 535 (1934).
- [18] W. G. Baber and H. R. Hassé, Proc. Cambr. Phil. Soc. **31**, 564 (1935).
- [19] D. R. Bates and T. R. Carson, Proc. Roy. Soc. London **A234**, 207 (1956).
- [20] Gisèle Hadinger, M. Aubert-Frécon, and Gerold Hadinger, J. Phys. **B22**, 697 (1989).
- [21] A. S. Davydov, *Quantum Mechanics*, 2nd edn. (Science, Moscow, 1973), Sects. 43, 118 (*in Russian*).
- [22] G. Holzwarth and H. J. Pfeiffer, Z. Phys. **A272**, 311 (1975).
- [23] A. V. Kravtsov, A. I. Mikhailov, and N. P. Popov, J. Phys. **B19**, 1323 (1986).
- [24] E. Clementi and C. Roetti, At. Data Nucl. Data Tables **14**, 177 (1974).